On the Kinematics of Sea-Land Breeze and the Local Development of Convective Storms in the Metropolitan Area of Rio de Janeiro

Sobre as Propriedades Cinemáticas da Brisa Marítima-Terrestre e o Desenvolvimento Local de Tempestades Convectivas na Região Metropolitana do Rio de Janeiro

Rodrigo Matola de Miranda Cardoso[1] ⓘ, Hugo Abi Karam[2] ⓘ,
José Paulo Soares de Azevedo[1] ⓘ

[1]Universidade Federal do Rio de Janeiro, Programa de Pós-Graduação em Engenharia Civil, Rio de Janeiro, RJ, Brasil
[2]Universidade Federal do Rio de Janeiro, Instituto de Geociências, Departamento de Meteorologia, Rio de Janeiro, RJ, Brasil
 E-mails: rodmatola@yahoo.com, hugo@igeo.ufrj.br, zepaulo@coc.ufrj.br
 Corresponding author: Hugo Abi Karam; hugo@igeo.ufrj.br

ABSTRACT

This work presents an analysis of the kinematic properties of the wind flow in the Metropolitan Area of Rio de Janeiro in the State of Rio de Janeiro, Brazil, using meteorological data from the aerodromes Santos Dumont, Galeão and Campo dos Afonsos, located in the city of Rio de Janeiro. The calculation of these kinematic quantities is based on the 'Linear Vector Point Function' (LVPF) method. The results indicate the main role of the circulation of the sea-land breeze, the effects of topography (by blockages, channeling and differential heating) and the urban breeze associated with the development of the Urban Boundary Layer in the local formation of convective rainstorms in the Metropolitan Area of Rio de Janeiro.

Keywords: Mesoscale circulations; Triggering of local storms; Linear Vector Point Function method

RESUMO

Este trabalho apresenta uma análise das propriedades cinemáticas do fluxo de vento na Região Metropolitana do Rio de Janeiro no Estado do Rio de Janeiro, Brasil, utilizando dados meteorológicos dos aeródromos Santos Dumont, Galeão e Campo dos Afonsos, localizados na cidade do Rio de Janeiro. O cálculo dessas quantidades cinemáticas é baseado no método 'Linear Vector Point Function' (LVPF). Os resultados indicam o papel principal da circulação da brisa mar-terra, dos efeitos da topografia (por bloqueios, canalização e aquecimento diferencial) e da brisa urbana associada ao desenvolvimento da Camada Limite Urbana na formação local de chuvas convectivas na Região Metropolitana do Rio de Janeiro.

Palavras-chave: Circulações de mesoescala; Desencadeamento de tempestades locais; Método da Função Pontual Vetorial Linear

1 Introduction

The Metropolitan Area of Rio de Janeiro (MARJ) presents the second biggest Brazilian urban area, with 22 municipalities (including the Capital), an area of 5.327 km^2 and 12,763,305 inhabitants. Geographically located between latitudes 22° 32' 14" S and 22° 54' 10" S and longitudes 42° 42' 51" W and 43° 42' 33" W, shows complex terrain with large urbanized area and several natural diversities. In the center of MARJ is located the Guanabara Bay (GB) (Figure 1).

Knowledge of local mesoscale circulations in the MARJ is still incomplete, despite the efforts made in research for the synoptic characterization of major extreme events in the area. For example, Jourdan, Marton and Pimentel (2006) and Pimentel et al. (2014) characterized the entry of the afternoon breeze into MARJ through climatological analysis based on wind roses, contributing to the knowledge of the surface flow and the atmospheric dispersion conditions of pollutants. Considering the distribution of precipitation in the Municipality of Rio de Janeiro, Dereczynski, Oliveira and Machado (2009) showed that the largest monthly

accumulations occur during the summer in mountainous terrain that permeates the urban area.

Moraes (2008), using simulations with the MM5 model, showed the importance of temperature advection and the development of the Urban Boundary Layer for defining wind flow in MARJ. The diurnal reversal of sea breezes to land breezes is easily noticeable in Sepetiba Bay, while the advection of the sea breeze is greatly intensified due to the coupling of the sea breeze circulations and the Urban Boundary Layer (UBL). The development of the UBL over the MARJ is marked by the development of very intense hot spots of surface heat and thermal disturbance in the vertical structure of the UBL, mainly in the "Baixada Fluminense" west of Guanabara Bay, associated with the formation of the spatial structure of the Urban Heat Island (UHI) on the MARJ.

Silva (2010) presented three-dimensional numerical simulations of UBL and UHI with the Brazilian Regional Atmospheric Modeling System (BRAMS) coupled to the Town Energy Budget (TEB) scheme, highlighting the importance of using the representation of urban canyons in the lower boundary condition in the model. In this way, obtained improved simulations not only of the spatial structure, but also of the temporal variation of both the UBL and the UHI, comparable to the knowledge available from MARJ. From sensitivity tests, showed that the urban surface scheme indeed improves the simulated results of maximum daytime temperatures. The joint analysis of the horizontal temperature and wind fields indicated that the TEB scheme allows simulating the spatial distribution of surface temperature hot spots in a manner consistent with the IHU observed at MARJ.

Observational extremes on temperature and precipitation trends were also obtained to support risk assessments and adaptations to climate change (Dereczynski, Luiz Silva & Marengo 2013), showing the climate in the Rio de Janeiro city has become more humid over forest surfaces and with heat waves have become longer. They also indicated that breezes and local moisture transport need to be further investigated in order to obtain a correct understanding of local meteorological conditions.
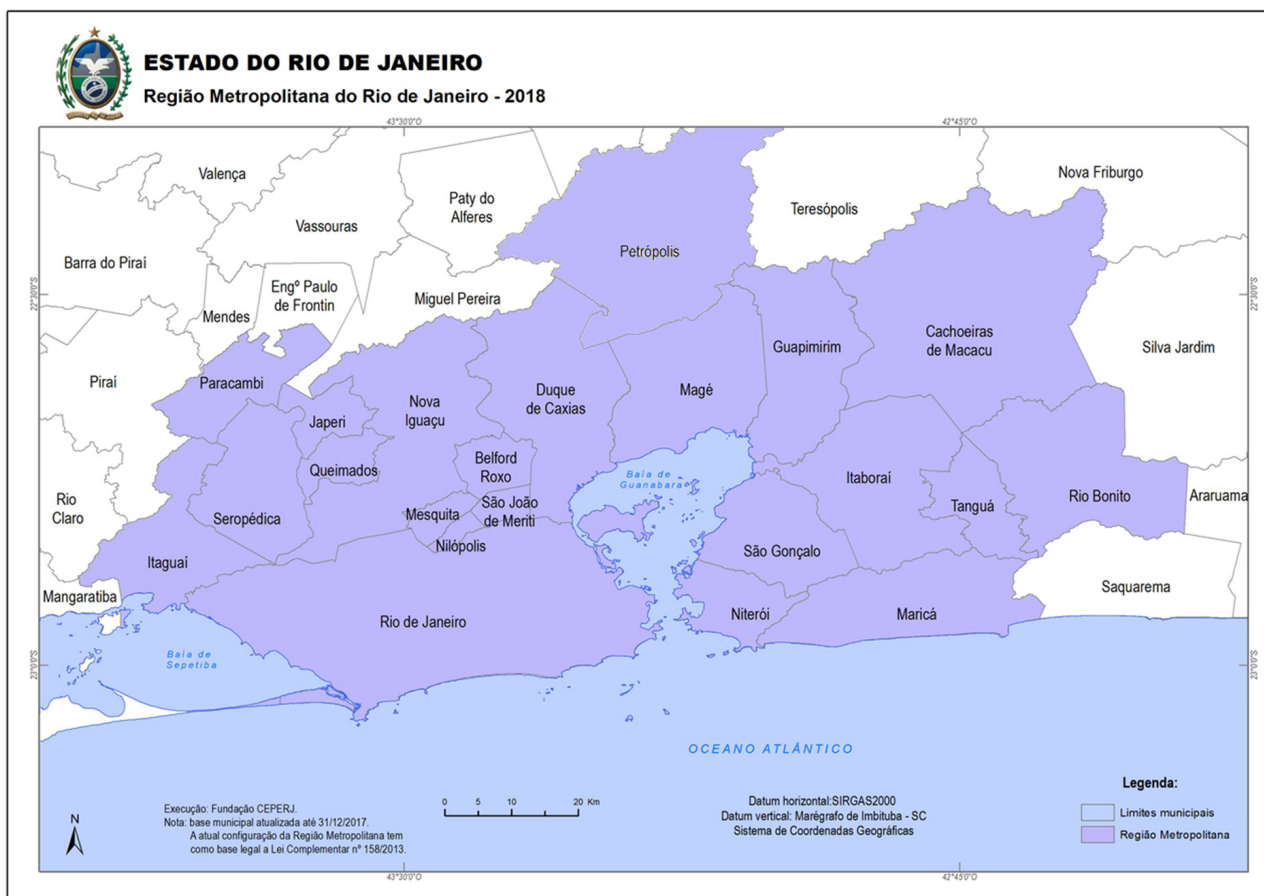

Figure 1 Metropolitan Area of Rio de Janeiro composed of 22 municipalities State of Rio de Janeiro, Brazil, including the municipality of Petrópolis according to Law No. 8674 of 20 Dec. 2019. Modified from the original by CEPERJ Foundation (2018).

Other investigations on the State of Rio de Janeiro (RJ) climate showed an increasing trend in annual rainfall for the coastal plain, lake region, and part of metropolitan area. Dry periods and intense rainfall likely tend to be concentrated in shorter and shorter periods. These results point to large increases in hydrometeorological and thermal hazards throughout the 21st century (Silva & Dereczynski 2014; Silva et al. 2014).

Associated with heavy precipitation events, synoptic analysis has showed the main role of wind divergence at 300 hPa, specific humidity distribution at 850 hPa, convective available potential energy (CAPE) and precipitable water along the troposphere (Polifke da Silva et al. 2015). Characterizing the intensity of rainfall, Pristo et al. (2018) showed that only 6.6 intense rainfall events, in accedence of 95% quantile, were responsible for 33% of the total average annual rainfall of the 32 available stations (1192 mm by year) in the Rio, distributed throughout the year, but predominantly in summer (43.7%).

Furthermore, Bonnet, Dereczynski and Nunes (2018) published climatological fields associated with intense post-frontal storms in the state of RJ, showing that events can be organized into three synoptic subgroups, according to the position of the frontal cloudiness band. Another research carried out by Escobar Marques and Dereczynski (2022) complemented the synoptic analysis of patterns of intense rainfall showing they are associated with the South Atlantic Convergence Zone (SACZ) and geopotential disturbances in 850 and 250-hPa, during prefrontal and frontal conditions. They showed that the first four principal components are associated with: a cyclone off the coast of RJ, a trough off the coast of RJ, high post-frontal pressures off the coast of RJ, and low pressures off the coast of the state of Santa Catarina, respectively.

In the Metropolitan Area of São Paulo (MASP) the interactions between breeze, urban boundary layer breezes and the local development of thunderstorms with hail during the late afternoon have been further investigated (Pereira Filho et al. 2004). The sea breeze strongly interacts with the Urban Boundary Layer, resulting in local storms over the urban area (Flores et al. 2019) or downwind of the urban area under the presence of synoptic forcings (Freitas et al. 2007; Silva Dias et al. 2013).

Lopez et al. (2023) published a work about the spatial analysis of the return period of daily extreme rainfall though the Serrana Zone of the State of RJ, using the objective analysis ANOBES applied to rainfall data and the Gumbel statistical distribution for analysis of extremes and return periods. These methods were applied to the mega disaster of 11 and 12 January 2011 in the Serrana Zone, that resulted in floods, landslides, erosion and many deaths. The results showed extremes of 240 mm per day at some locations in the Serrana Zone, with return periods of 100-years or more. On 11 January 2011, cumulative rainfall volume was high (>100 mm), but on January 12 it was extreme, similar to 100-year return time data.

For MARJ, Sousa and Karam (2014) showed that intense southerly winds or a sudden change in wind direction from west to southwest associated with post-frontal conditions and ocean cyclogenesis to the south can trigger strong storms on the slopes of Serra do Sea (SM) causing large volumes of rain in the Serrana Zone or its surroundings.

An open question for research is whether the intensification of the sea breeze in the afternoon at MARJ (Figure 1) could be responsible for triggering or intensifying the storms along the northern edge of GB, where the slopes of Serra do Mar are also located?

From a theoretical point of view, advection and convergence are best known in the literature for their association with early and mature stages of storm cell development (e.g., Bluestein 1992). The interaction between sea, urban and convective breeze circulations is still little known in South America, and it is particularly true in MARJ, where the urban heat island is segmented by the presence of the GB and by three massive granitic outcrops.

We will approach this question in this work detailing the kinematic properties (velocity and direction, vorticity, divergence and deformations) of the surface wind field following Zamora, Shapiro and Doswell III (1987) and Doswell (1984). This work presents the analysis of wind kinematics in MARJ based on the Linear Vector Point Function (LVPF), following the matrix formalism described by Zamora, Shapiro and Doswell III (1987).

2 Data and Analysis Method

Meteorological stations data from MARJ Santos Dumont, Galeão and Campo dos Afonsos airports (Table 1), sampled every hour, were pooled and then paired to obtain a flawless series, between July 1996 and March 2009, corresponding to a period of approximately 13 years.

The data were used to calculate averages and variances for every hour of every 15 days over the average year. The result obtained is a first-order approximation of surface wind climatology. Next, the average wind values were applied in the LVPF method to obtain the kinematic properties of surface wind flow. Finally, the kinematic properties were plotted and analyzed.

Table 1 Coordinated positions of airport weather stations in MARJ.

Weather Stations (METAR code)	Latitude (deg min sec)	Longitude (deg min sec)	Altitude (m)
SBRJ	-22° 54' 38" S	-43°09'47" W	3
SBGL	-22° 48' 32" S	-43°14'37" W	9
SBAF	-22° 52' 30" S	-43°23'05" W	34

2.1 Kinematics of Wind Flow

Following Saucier (1955) and Petersen (1956), let's be a coordinated point (x,y) in the vicinity of the point (x0,y0) and displacement components given by $\delta x = (x-x_0)$ and $\delta y = (y-y_0)$. The horizontal wind components of the surface wind $V=(u,v)$ can be expressed by Taylor series expansions around (x0,y0), as shown in Equation 1.

$$u(x,y)=u_0 + \frac{\partial u}{\partial x}\delta x + \frac{\partial u}{\partial y}\delta y + \cdots$$
$$v(x,y)=v_0 + \frac{\partial v}{\partial x}\delta x + \frac{\partial v}{\partial y}\delta y + \cdots \tag{1}$$

where $u_0=u(x_0,y_0)$ and $v_0=v(x_0,y_0)$ are the wind components to (x_0,y_0). Then, neglecting the second and higher order terms in the Taylor expansion it is obtained the first order linear approximation. The kinematics properties of wind flow (stretching deformation, shearing deformation, divergence and vorticity) are expressed by Equation 2.

$$\text{def}V \equiv 2a = \frac{\partial u}{\partial x} - \frac{\partial v}{\partial y}, \text{def '}V \equiv 2a' = \frac{\partial v}{\partial x} + \frac{\partial u}{\partial y}$$
$$\text{div}V \equiv 2b = \frac{\partial u}{\partial x} + \frac{\partial v}{\partial y}, \text{rot}V \equiv 2c = \frac{\partial v}{\partial x} - \frac{\partial u}{\partial y} \tag{2}$$

The linearized form of the wind components in the vicinity of the point are given in Equation 3.

$$u \approx u_0 + a\delta x + a'\delta y + b\delta x - c\delta y$$
$$v \approx v_0 - a\delta y + a'\delta x + b\delta y + c\delta x \tag{3}$$

where $u_0=u(x_0,y_0)$ and $v_0=v(x_0,y_0)$.

Zamora, Shapiro and Doswell III (1987) proposed a direct method to obtain the values of u_0, v_0, a, a', b and c. The method correspond to a optimization, considering the known vectors $X=(x_1, y_1, x_2, y_2, x_3, y_3)$, the observation vector $U=(u_1, v_1, u_2, v_2, u_3, v_3)$, and the incognitos vector $D=(u_0, v_0, a, a', b, c)$. The matricial form is shown in Equation 4.

$$DX=U \tag{4}$$

where $X_{6\times6}$ is the matrix of coefficients, which is given by Equation 5.

$$X=\begin{pmatrix} 1 & 0 & 1 & 0 & 1 & 0 \\ 0 & 1 & 0 & 1 & 0 & 1 \\ \partial x_1 & -\partial y_1 & \partial x_2 & -\partial y_2 & \partial x_3 & -\partial y_3 \\ \partial y_1 & \partial x_1 & \partial y_2 & \partial x_2 & \partial y_3 & \partial x_3 \\ \partial x_1 & \partial y_1 & \partial x_2 & \partial y_2 & \partial x_3 & \partial y_3 \\ -\partial y_1 & \partial x_1 & -\partial y_2 & \partial x_2 & -\partial y_3 & \partial x_3 \end{pmatrix} \tag{5}$$

In Equation (5) the metrics are $\delta x_i=(x_i-x_0)$ and $\delta y_i=(y_i-y_0)$, which are obtained as distances between three non-collinear points. Finally, the solution can be obtained by Equation 6.

$$D=UX^{-1} \tag{6}$$

in which the observation vector is multiplied by the inverse of the coefficient matrix.

3 Results

The kinematic wind properties were computed around the barycenter of the weather station triangle shown in Figure 2A. A circular neighborhood with radius given by the average distance between stations is considered here. The results computed strictly within the circular neighborhood of the barycenter can be considered representative of conditions on the western edge of the urban surface of Guanabara Bay (GB). Due to the symmetry with the opposite shore of GB, the hypothesis of a mirrored field in the other location cannot be ignored. It is worth highlighting the role of the meridional wind from the south in the afternoon due to the acceleration of the sea breeze between 12:00 and 16:00 LT and deceleration between 16:00 and 24:00 LT (Figure 2B). Vectors rotate counterclockwise in both sides of GB due to inertial oscillation. Considering the abrupt elevation of the topography to the north of the bay, a convergence of the sea breeze front is expected along the northern edge of GB.
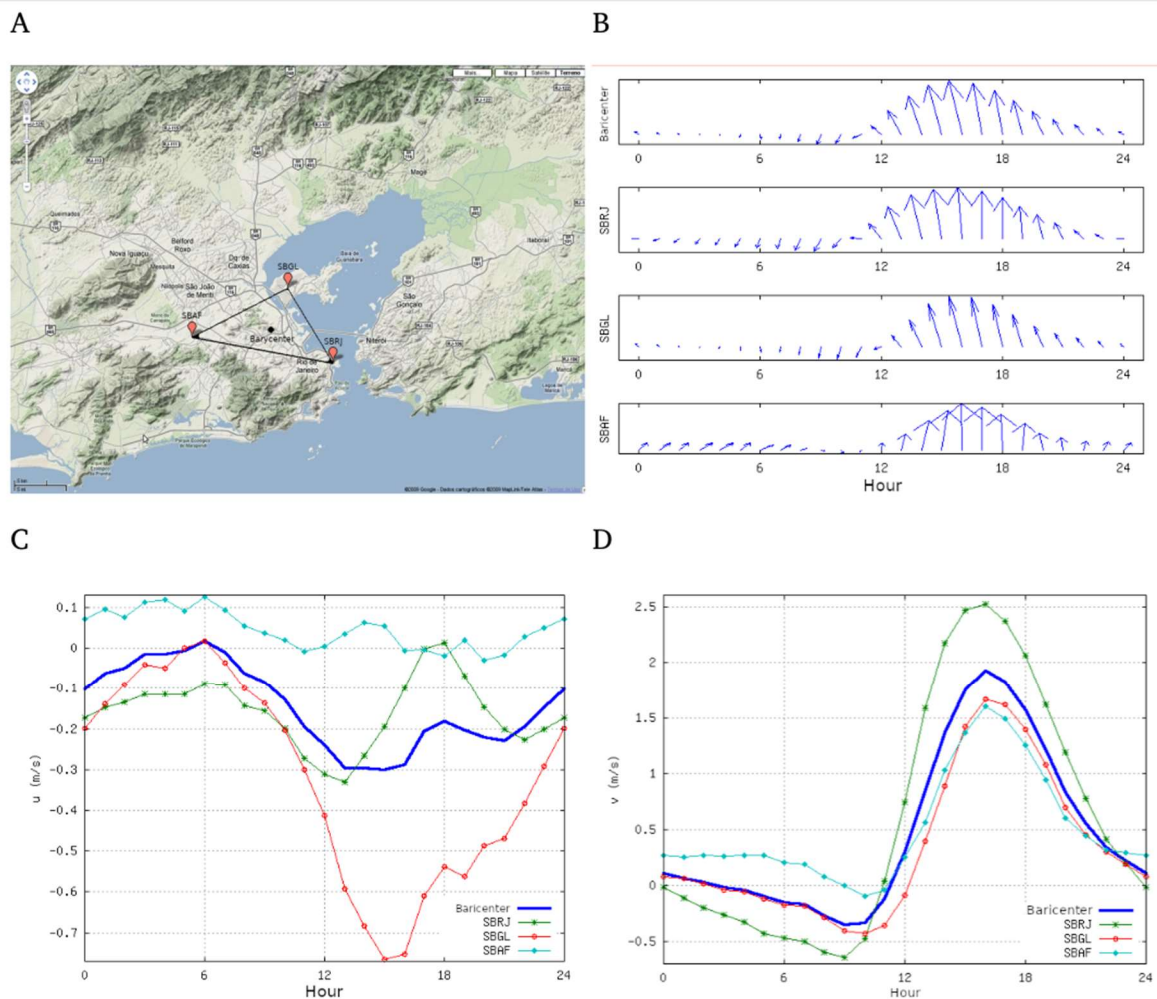
Figure 2 A. Location of the three airports in MARJ; B. Evolution of the average wind vector for the meteorological stations SBRJ, SBGL, SBAF and barycenter (the maximum magnitude of the vectors is 2.5 m s⁻¹); C. Temporal evolution of the hourly average of the zonal wind component in (m s⁻¹); D. The same for the meridional component in (m s⁻¹).

The graphs of the 24 hour evolution of the zonal and meridional components of the wind are shown in Figures 2C and 2D. The hourly behavior of the zonal component is not as wavy as that observed in the meridional component, mainly due to the effects of urban surface elements (i.e., buildings, hills, roads, vegetation and urbanization patterns that can block or channel airflow).

As the Campos dos Afonsos meteorological station is inserted in the western conurbation and the Santos Dumont station is located in the Historic Port Zone of the city of Rio de Janeiro, a channeling of the wind flow is likely to be considered the alignment of the flow by the most frequent direction of public roads and south-north orientation of the facades of the buildings, along the edge of GB. As a result, the longitudinal axis of GB provides a free path for the transport of air parcels by the meridional breeze component.

The climatological proxy of the mean zonal and meridional wind components along the year for SBGL weather station are shown in Figures 3A and 3B. The period used to obtain the climatology is approximately 13 years (from July 1996 to March 2009). In the afternoon, the zonal wind component (Figure 3A) shows the breeze blowing from the east, from GB towards the city to the west, except in July (winter solstice in the Southern Hemisphere).

In winter, the meridional component decreases slightly in the afternoon (Figure 3B), while the zonal component becomes positive with low intensity during the night. This is caused by the reduction of surface thermal contrast, compared to summer values.
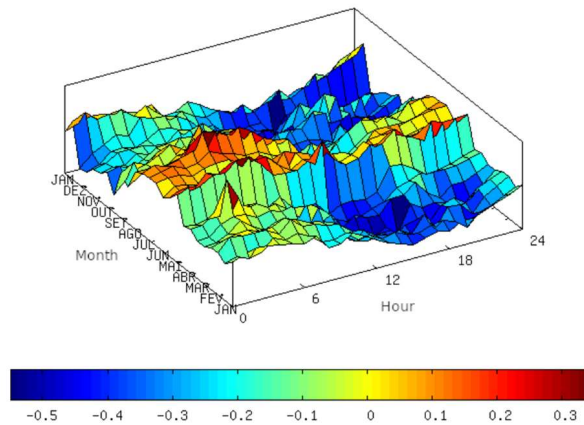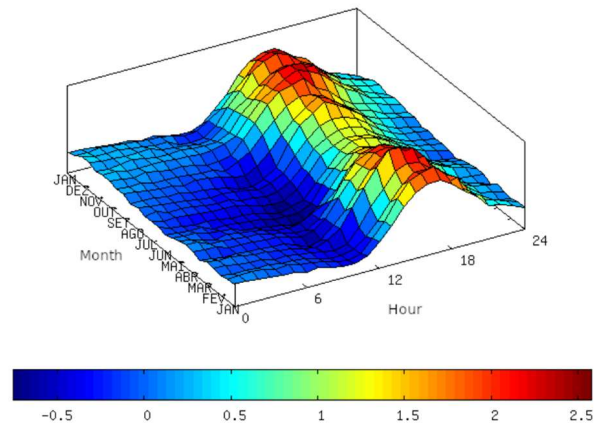
A - Zonal component (m s⁻¹)   B - Meridional component (m s⁻¹)

Figure 3 Climatology of the magnitude of wind components in (m s⁻¹) at the SBGL station: A. Zonal component; B. Meridional component. Period: from July 1996 to March 2009. The magnitude is shown by the key scale.

Throughout the year, the meridional wind distribution within the triangular area os weather stations is primarily responsible for local flow convergence. The convergence extends to the Serra do Mar slopes north of the bay, since the horizontal wind speed is zero over any topographical surface, the extent of breeze convergence in the urban area is an empirical result.

The distribution of the south meridional component shows persistence throughout the year. The afternoon south breeze, observed throughout the year, may be the result of the interactions and coupling of sea, urban and valley-mountain breezes, which together form the lower branch of a shallow circulation cell.

In a complementary way, the Afonsos station (SBAF) presents a very weak zonal wind from the west in the late afternoon, reflecting the effect of the geometry of the coastline and also the topographic baroclinic forcing, which defines a thermal gradient to the northeast.

Surface heterogeneities, associated with the distribution of vegetation, urban areas, water surfaces and relief, generate surface gradients of sensible and latent heat fluxes. In this way, the flow of the lower branch of the circulation is responsible for the transport (advection) of heat and water vapor from one point to another. Particularly, the air parcels can be transported along the GB corridor to the northern areas, close to the Serra do Mar slopes, where local storms are likely to form.

The average distribution of wind kinematic properties over the days of the year and hours of the day is shown in Figure 4. The results show that throughout the year there is a predominance of negative divergence (i.e., convergence) during the afternoon, while the sea breeze accelerates from south to north (Figure 4A). At night, the magnitude of the divergence decreases to around zero, probably due to the reversal of direction from the sea breeze to the land breeze.

The convergence of the sea breeze in the afternoon is due to the deceleration of the flow caused by the mechanical and thermal effects of the topography. This convergence, associated with the advection of heat and humidity through the flow of sea and urban breezes, leads to conditions that favor the triggering of thunderstorms over hot spots in the urban heat island and downwind.

The degree of nocturnal divergence can be associated with slower evolution of the land breeze. Land breeze velocity can increase if urban surface temperatures fall below 22.5°C, which is the average sea surface water temperature along the coast of the State of Rio de Janeiro (Reynolds & Smith 1995). Furthermore, under clear sky conditions, katabatic winds may likely develop on slopes, with downwind convergence.

The average vorticity is predominantly positive during the day (Figure 4B), being negative only in spring, in the same period. This may be related to: 1) the inclination of the horizontal vorticity tubes that form in the surface boundary layer due to the effect of differential topographic elevation; 2) increase in surface roughness as the flow advances from east to west from the central corridor of GB; and 3) divergence of the breeze associated with the curved geometry of GB and the counterclockwise deviation due to the inertial acceleration of the sea breeze flow during its afternoon development.
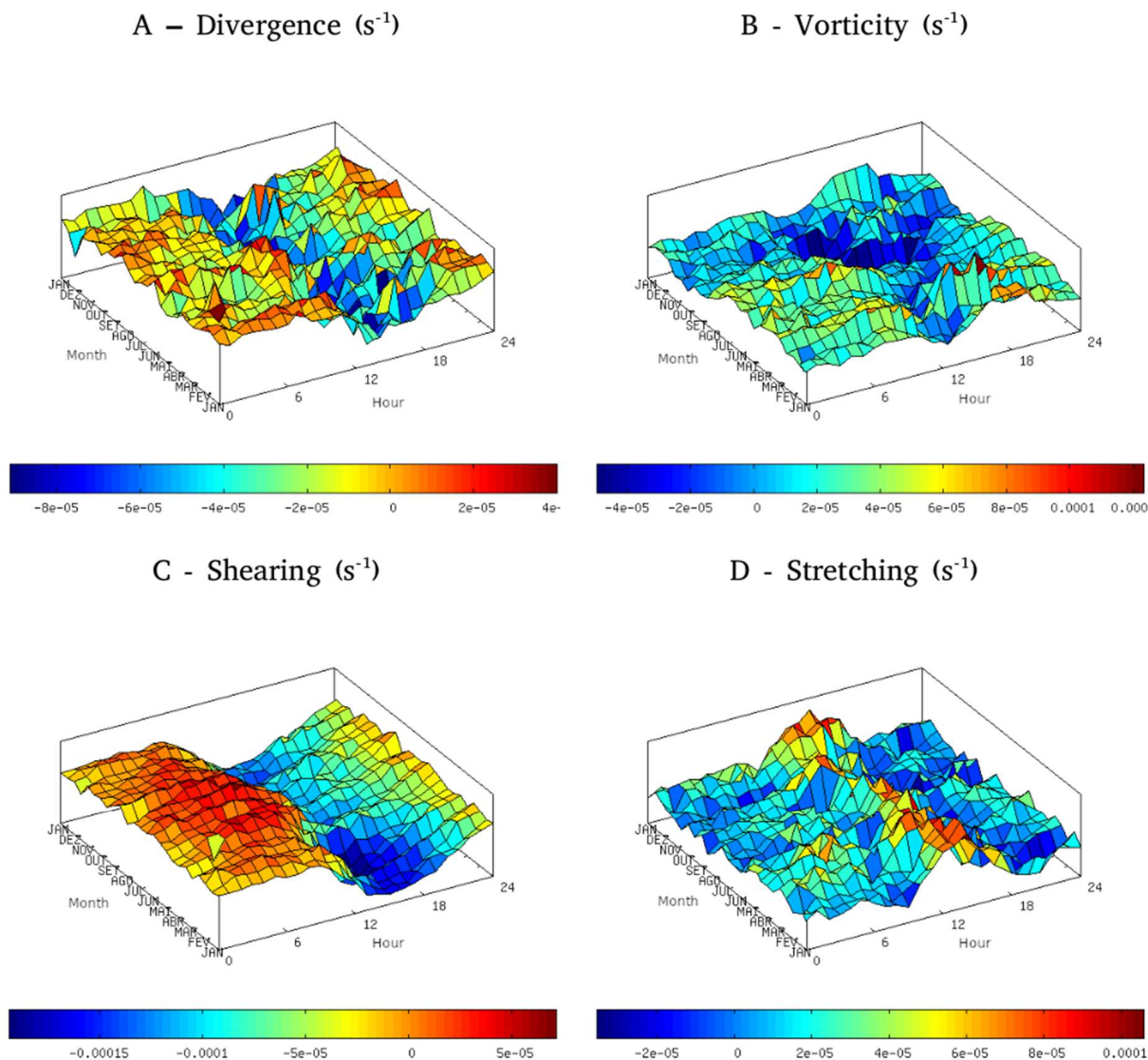
A – Divergence (s⁻¹)

B - Vorticity (s⁻¹)

C - Shearing (s⁻¹)

D - Stretching (s⁻¹)

Figure 4 Wind kinematic properties in units of (s⁻¹) obtained with LVPF method in the west border of GB of Rio de Janeiro. The plots correspond to: A. Divergence; B. Vorticity; C. Shearing; D. Stretching of the surface wind flow.

The effect of counterclockwise rotation of the wind breeze vector throughout the day is remarkable, not explicitly pointed out in previous works based on compass roses, probably because the roughness of the urban surface and the presence of topography, inside and outside the urban area, can significantly change the flow direction locally. At noon, the acceleration of the sea breeze increases the flow first at Santos Dumont airport and then at Galeão. At the end of the afternoon, the behavior of the wind in both seasons is quite similar, probably due to the spreading of the sea breeze front on both sides of GB.

The deformation occurs in association with the sea-land breeze circulation (Figures 4C and 4D). Shear occurs at the same time as the incoming sea breeze from 11:00 LT until midnight. During this period, the lower branch of the breeze circulation undergoes shear on both sides of GB, that also acts as an atmospheric corridor for the entry of sea breezes during the afternoon and early evening. During dawn and morning, it acts as an atmospheric corridor for the outflow of terrestrial, urban and mountain-valley breezes. In the afternoon, the air parcels of the lower branch of the sea breeze accelerate due to flow stretching, i.e., in the absence of other more intense forcings.

The inertial period of the breeze circulation in Rio de Janeiro is greater than 24 hours, which causes a progressive lag in the intensity of the sea breeze in relation to the

diurnal cycle associated with the heating of the slopes and the urban heat island. After a sequence of days, both cycles enter a phase and more intense breeze events can occur. Conceptually, both lateral shear and longitudinal wind stretching of the sea breeze can intensify the vertical component of vorticity.

3.1 Case Study (Thunderstorm Triggering by Sea Breeze in MARJ)

On 02/24/2010, an intense convective condition develops in MARJ associated with prefrontal squall lines aligned from SE to SW, during the late afternoon, has been evidenced by perturbations in the surface variables (Figure 5) and by maxCAPPI images from Pico do Couto radar (Figure 6).

From 5:00 pm to 9:00 pm LT, radar shows convective storm formation in an arc shape around GB to the north, extending along the ridge (Figure 6). Later, the clouds arrive near GB, a few hours before the cold front. The source of moisture in the system is the southerly breeze, entering around 16:00 LT at Santos Dumont airport (SBRJ station) and 16:30 LT at Galeão airport station (SBGL), with a velocity of 8 m s^{-1} (Figure 5). The observed maximum dew point temperature showed a high value of 36°C, which increased the buoyancy of the surface air parcels.

As previously pointed out, the increase in south wind speed associated with the breeze is a common event, as confirmed by weather station data. On this day, an increase in wind speed from 19 to 35 km h^{-1} was recorded, associated with the wind turning from south to north twice, the first at 15:30 LT and the second at 18:00 LT.
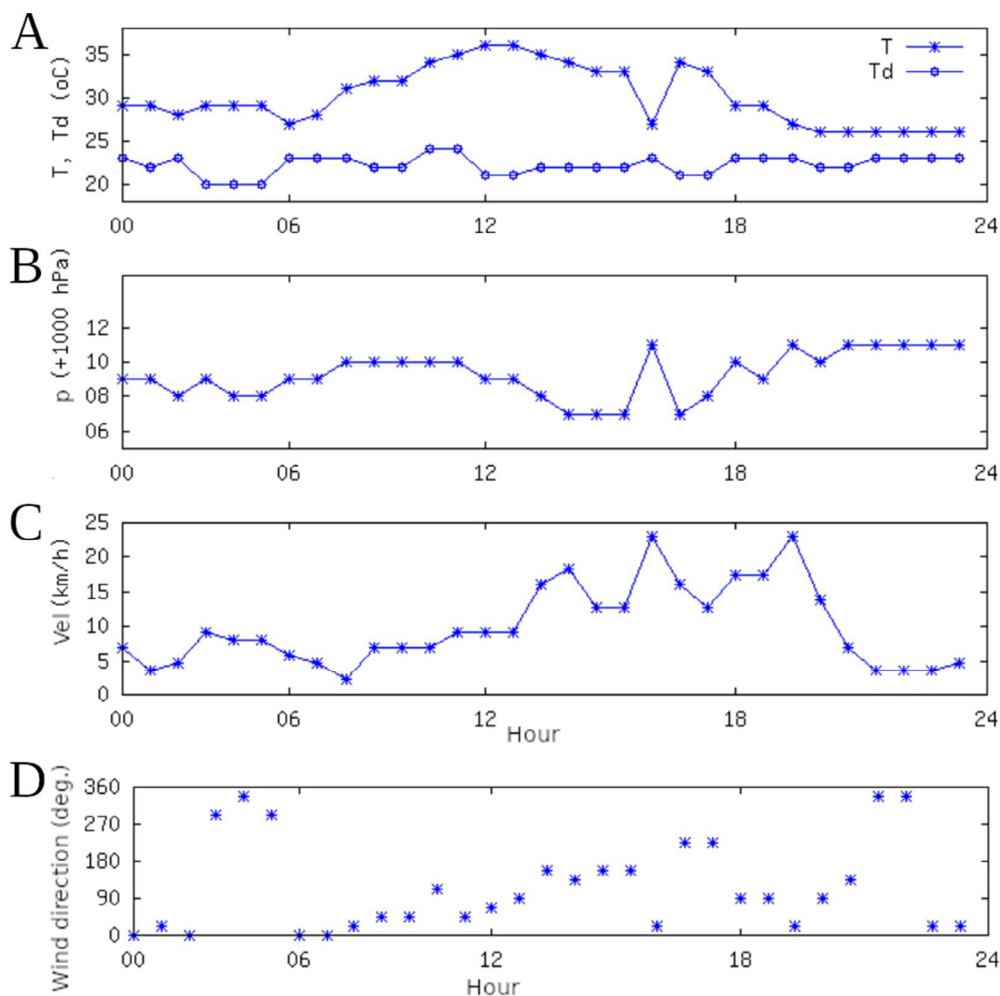

Figure 5 Diurnal evolution of surface meteorological variables, plotted from METAR data from 02/24/2010, from the meteorological station at Galeão Airport (SBGL): A. Air temperature T (°C) and dew point temperature Td (°C), B. Atmospheric pressure p (+1000 hPa); C. Wind speed Vel (km h-1); D. Wind direction (azimuth) (degrees). The time axis (in hours) shows local time (LT).
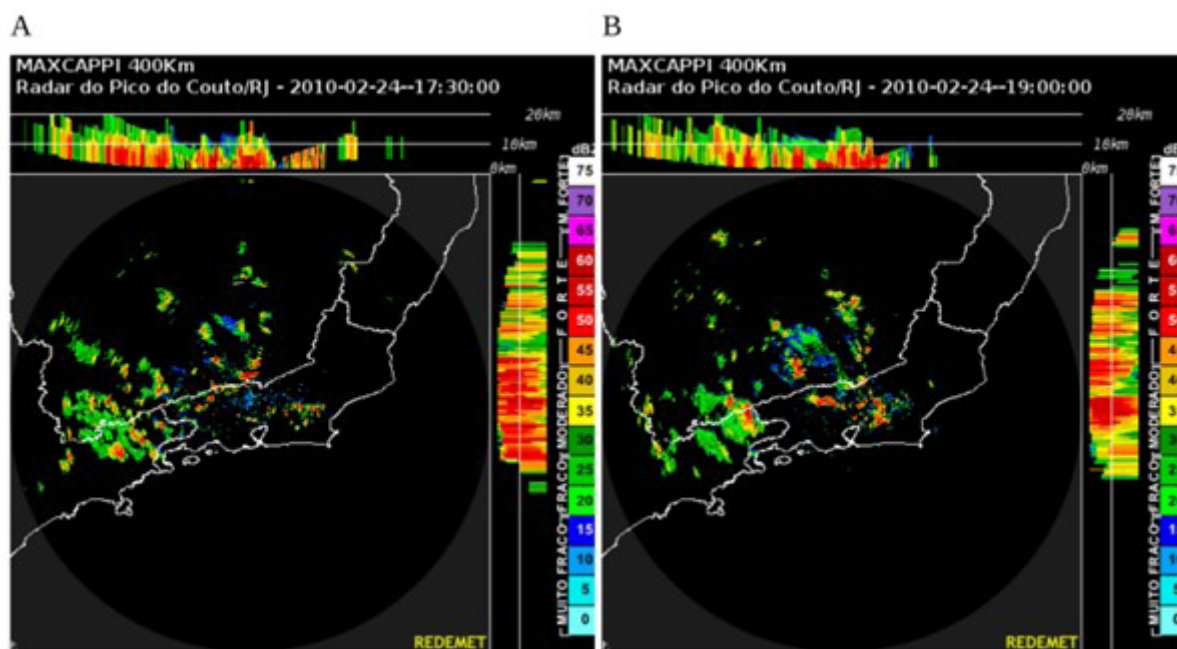
Figure 6 Radar images (maxCAPPI) from Pico do Couto band-S weather radar: A. At 14:30 LT; B. At 16:00 LT of 02/24/2010.

This increase in wind results in an increase in dynamic, non-hydrostatic pressure, with a value between 2 and 4 hPa, and a decrease in temperature of 6°C.

These sub-hourly variations are probably associated with the passage of gust fronts originating in the downdrafts of the storm cells. These disturbances were recorded over a period of no more than one hour, not being associated with variations due to the daily oscillation of the breeze circulation (i.e., in the opposite direction of the sea breeze, at the time).

The hourly transients seem to be associated with the propagation of an internal gravity wave or even with the passage of a density current originated during the mature stage of the storm. The disturbances are recorded after the maximum convective development of the storm that occurs at the bottom of GB.

The analysis of the event raises the following question. If the breeze front can propagate more easily to the east or west from the central axis of GB? A fact in favor of the preferential trajectory towards the east is associated with the blockage of flow by the hills to the west, the presence of Governor Island and its rugged terrain and the low river plain of the Environmental Protection Area (APA) of Guapimirim, to the east. If this hypothesis is confirmed in the future, the convergence areas can be induced preferentially to the northeast of the Bay, favoring the initial development of storms in the region.

The hydrographic basin of APA Guapimirim (composed of mountain ranges and mangrove area) is another hydrometeorological indicator of preferential location for the formation of rainfall in the boundaries of MARJ. Storms with local development associated with the convergence of breeze fronts can be observed in the absence of other important synoptic forcings, in summer prefrontal conditions. Favorable areas for these storms are likely to the north and northwest of GB (as exemplified in the case study of Figure 6).

Additionally, the observational analysis allowed describing the diurnal and seasonal cycles of vertical vorticity in the urban area west of GB. A positive component occurs during the afternoon, indicating a counterclockwise rotation of the wind field to the west of the bay, which may be associated with the shear of the breeze wind field and the inclination of vortex tubes as the flow rises in the slopes of the hills in the afternoon (Figure 7).

4 Conclusions

This work presents evidences of interactions between mesoscale circulations (sea-land breeze, mountain-valley breeze and urban breeze) in the Metropolitan Area of Rio de Janeiro and the triggering of local storms north of GB. Diurnal cycles of convergence, vorticity, shear and wind field stretching were diagnosed from hourly climatology.
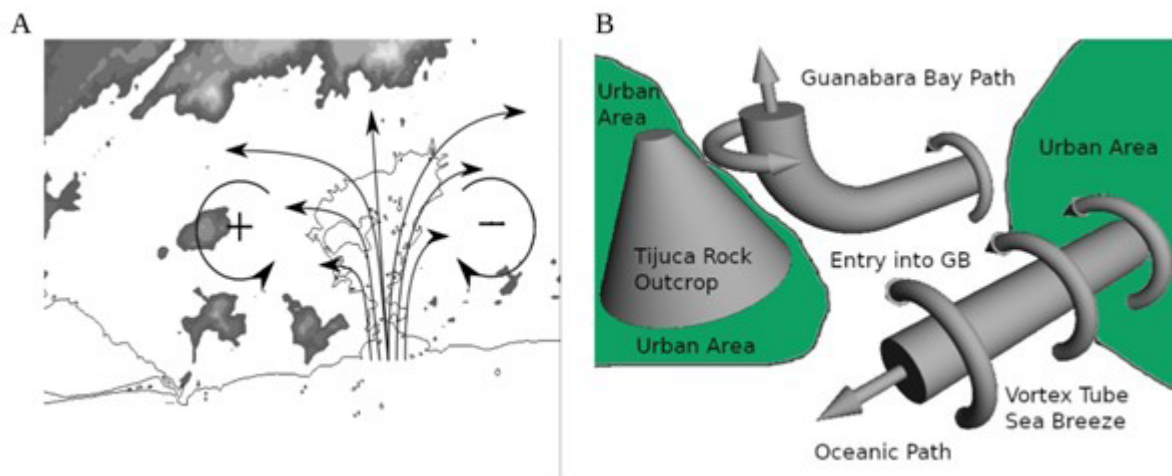
Figure 7 Conceptual model of sea breeze surface flow associated with the geometry of the edge of the GB and the rocky outcrops west of the GB in MARJ: A. Illustration of the divergence and rotation effects of sea breeze surface flow due to the geometry of the bay edge; B. Illustration of the tilting effect of a vortex tube, which originally had only a horizontal component, as it passed over an idealized hill with a conical-shaped rocky outcrop, west of the entrance to Guanabara Bay. In B, the idealized topography of the conical hill represents a rocky outcrop to the west of GB.

The associated surface meteorological fields are consistent with daily oscillation of mesoscale circulations (breezes) but also with lag of the local inertial oscillation in relation to the daily cycle.

The mechanical effects of topography such as channeling, blocking and flow elevation also seem to play a relevant role in the absence of relevant synoptic forcing. The surface flow convergence may also be associated with the change in aerodynamic roughness as sea air parcels pass from the smooth water surface to the rough urban surface. Sea breeze flow carries relatively cool, moist air to areas more or more favorable for storm surges. A conceptual model emerges from the presented analysis. In this, the GB is the main atmospheric corridor for the entry and exit of sea and land breezes (i.e., together with Sepetiba Bay to the west), in the absence of larger synoptic forcings.

The change in surface roughness, the daily evolution of the urban heat island and the presence of topography on the sides and bottom of the GB seem to be associated with the convergence-divergence of the flow along the south-north axis of the bay, at the same time as causes shear, stretching and vorticity in the urban areas of the lateral margins. Finally, areas of convergence to the north and in the urban and natural areas on the sides of GB can conceptually be preferred areas for the triggering of intense convective storms associated with the breeze at MARJ.

The present evidence corroborates the a conceptual model of precipitation for MARJ (e.g., Santos 2019), which has proposed three main precipitation patterns for the State of Rio de Janeiro: type I: mesoscale convective systems (i.e., associated with squall lines and clusters of storms with eastward group velocity), type II: interactions of mesoscale circulations associated with sea-land, urban, and valley-mountain breezes, flow convergence, barrier blockage, channeling of the relief and baroclinic effects, and type III: precipitation associated with the passage of cold fronts.

Following this work, there is the possibility of applying numerical mesoscale models to investigate the development of intense rainfall in the Metropolitan Area of Rio de Janeiro, as applied by Freitas et al. (2007) and Flores Rojas et al. (2019) to simulate the UBL and UHI of the Metropolitan Area of São Paulo. Such modeling would allow assessing details of the relative importance of different physical mechanisms associated with the development of storms on complex terrain (e.g., He et al. 2023).

5 Acknowledgments

6 References

Bluestein, H.B. 1992, *Synoptic-Dynamic Meteorology in Midlatitudes*: *Vols. I and II. Principles of Kinematics and Dynamics*, Oxford University Press, Oxford.

Bonnet, S.M., Dereczynski, C.P. & Nunes, A. 2018, 'Caracterização sinótica e climatológica de eventos de chuva pós-frontal no Rio de Janeiro', *Revista Brasileira de Meteorologia*, vol. 33, no. 3, pp. 547-57, DOI:10.1590/0102-7786333013.

CEPERJ 2018, *Mapa Da Região Metropolitana do Rio de Janeiro*, Fundação Centro Estadual de Estatísticas, Pesquisas e Formação de Servidores do Rio de Janeiro.

Dereczynski, C.P., Oliveira, J.S. & Machado, C.O. 2009, 'Climatologia da precipitação no município do Rio de Janeiro', *Revista Brasileira de Meteorologia*, vol. 24, no. 1, pp. 24-38, DOI:10.1590/S0102-77862009000100003.

Dereczynski, C.P., Luiz Silva, W. & Marengo, J.A., 2013, 'Detection and projections of climate change in Rio de Janeiro, Brazil', *American Journal of Climate Change*, vol. 2, pp. 25-33, DOI:10.4236/ajcc.2013.21003.

Doswell, C.A. 1984, 'A kinematic analysis of frontogenesis associated with a nondivergent vortex', *Journal of the Atmospheric Sciences*, vol. 41, no. 7, pp. 1242-8, DOI:10.1175/1520-0469(1984)041%3C1242:AKAOFA%3E2.0.CO;2.

Escobar, G.C.J., Marques, A.C.A. & Dereczynski, C.P. 2022, 'Synoptic patterns of South Atlantic Convergence Zone episodes associated with heavy rainfall events in the city of Rio de Janeiro, Brazil', *Atmósfera*, vol. 35, no. 2, pp. 287-305, DOI:10.20937/ATM.52942.

Flores Rojas, J.L., Pereira Filho, A.J., Karam, H.A., Vemado, F., Masson, V. & Silva-Vidal, F.Y. 2019, 'Modeling the effects of explicit urban canopy representation on the development of thunderstorms above a tropical mega city', *Atmosphere*, vol. 10, no. 7, 356, DOI:10.3390/atmos10070356.

Freitas, E.D., Rozoff, C.M., Cotton, W.R. & Dias, P.L.S. 2007, 'Interactions of an urban heat island and sea-breeze circulations during winter over the metropolitan area of São Paulo, Brazil', *Boundary-Layer Meteorology*, vol. 122, pp. 43-65, DOI:10.1007/s10546-006-9091-3.

He, X., Abulikemu, A., Mamtimin, A., Li, R., Abulimiti, A., An, D., Aireti, M., Zhou, Y., Sun, Q., Li, Z. & Yuan, L. 2023, 'On the mechanisms of a snowstorm associated with a low-level cold front and low-level jet in the Western Mountainous egion of the Junggar Basin, Xinjiang, Northwest China', *Atmosphere*, vol. 14, no. 6, 919, DOI:10.3390/atmos14060919.

Jourdan, P., Marton, E. & Pimentel, L.C. 2006, 'Caracterização do regime de vento próximo à superfície na Região Metropolitana do Rio de Janeiro no período 2002-2006', *Proceedings of XIV Congresso Brasileiro de Meteorologia*.

Lopez, M.D.C.S., Pinaya, J.L.D., Pereira Filho, A.J., Vemado, F.L. & Reis, F.A.G.V. 2023, 'Analysis of Extreme Precipitation Events in the Mountainous Region of Rio de Janeiro, Brazil', *Climate*, vol. 11, no. 3, 73, DOI:10.3390/cli11030073.

Moraes, N.O. 2008, 'Caracterização do regime de vento em superfície na Região Metropolitana do Rio de Janeiro', Master's thesis, Federal University of Rio de Janeiro, Brazil.

Petersen, S. 1956, *Weather Analysis and Forecasting. Vol. I: Motion and Motion Systems*, 2nd edn, McGraw-Hill, New York.

Pereira Filho, A.J., Barros, M.T.L., Hallak, R. & Gandu, A.W. 2004, 'Enchentes na Região Metropolitana de São Paulo: aspectos de mesoescala e avaliaçao de impactos', *Proceedings of XIII Congresso Brasileiro de Meteorologia*, Rio de Janeiro.

Pimentel, L.C.G., Marton, E., Silva, M.S. & Jourdan, P. 2014, 'Caracterização do regime de vento em superfície na Região Metropolitana do Rio de Janeiro', *Engenharia Sanitária e Ambiental*, vol. 19 no. 2, pp. 121-32, DOI:10.1590/S1413-41522014000200003.

Polifke da Silva, F., Justi da Silva, M. G. A., Menezes, W. F. & Almeida, V. A. 2015, 'Avaliação de Indicadores Atmosféricos Utilizando o Modelo Númerico WRF em Eventos de Chuva na Cidade do Rio de Janeiro', *Anuário do Instituto de Geociências*, vol. 38, no. 2, pp. 81-90, DOI:10.11137/2015_2_81_90.

Pristo, M.V.J., Dereczynski, C.P., Souza, P.R. & Menezes, W.F. 2018, 'Climatologia de chuvas intensas no município do Rio de Janeiro', *Revista Brasileira de Meteorologia*, vol. 33, no. 4, pp. 615-30, DOI:10.1590/0102-7786334005.

Reynolds, R.W. & Smith, T.M., 1995, 'A high-resolution global sea surface temperature climatology'. *Journal of Climate*, vol. 8, no. 6, pp. 1571-1583.

Santos, G.R.D. 2019, 'Climatologia horária da estação meteorológica do Aeroporto Internacional do Rio de Janeiro: uma contribuição ao estudo do clima urbano', Master's thesis, Federal University of Rio de Janeiro, Brazil.

Saucier, W.J. 1955, *Principles of Meteorology Analysis*, University of Chicago Press, Chicago.

Silva Dias, M.A., Dias, J., Carvalho, L.M., Freitas, E.D. & Silva Dias, P.L. 2013, 'Changes in extreme daily rainfall for São Paulo, Brazil', *Climatic Change*, vol. 116, pp. 705-22, DOI:10.1007/s10584-012-0504-7.

Silva, F.B. 2010, 'Estudo de ilha de calor na região metropolitana do Rio de Janeiro: aspectos das circulações locais com utilização do modelo atmosférico BRAMS', Master's thesis, Federal University of Rio de Janeiro, Brazil.

Silva, W.L. & Dereczynski, C.P. 2014, 'Caracterização climatológica e tendências observadas em extremos climáticos no estado do Rio de Janeiro', *Anuário do Instituto de Geociências – UFRJ*, vol. 37, no. 2, pp. 123-38, DOI:10.11137/2014_2_123_138.

Silva, W.L., Dereczynski, C.P., Chou, S.C. & Cavalcanti, I. 2014, 'Future Changes in Temperature and Precipitation Extremes in the State of Rio de Janeiro (Brazil)', *American Journal of Climate Change*, vol. 3, pp. 353-65, DOI:10.4236/ajcc.2014.34031.

Sousa, F.B.B. & Karam, H.A. 2014, 'Análise da estrutura termodinâmica associada ao desenvolvimento de tempestade ocorrida entre 17 e 18 de março de 2013 no Estado do Rio de Janeiro, Brasil', *Anuário do Instituto de Geociências*, vol. 37, pp. 17-26, DOI:10.11137/2014_1_17_26.

Zamora, R.J., Shapiro, M.A. & Doswell III, C.A. 1987, 'The diagnosis of upper tropospheric divergence an ageostrophic wind using profiler wind observations', *Monthly Weather Review*, vol. 115, no. 4, pp. 871-84, DOI:10.1175/1520-0493(1987)115%3C0871:TDOUTD%3E2.0.CO;2.

Author contributions
Rodrigo Matola de Miranda Cardoso: project design; project plan; conceptualization; formal analysis; methodology; numerical implementation; verification-validation; writing-original draft; writing, review and editing; visualization and discussions. **Hugo Abi Karam:** project design; project plan; conceptualization; formal analysis; methodology; numerical implementation; verification-validation; writing-original draft; writing, review and editing; visualization and discussions. **José Paulo Soares de Azevedo:** formal analysis; verifications and discussions.

Conflict of interest
The authors declare no conflict of interest.

Data availability statement
Reference datasets, scripts and code are available on request.

Editor-in-chief
Dr. Claudine Dereczynski

Associate Editor
Dr. Fernanda Cerqueira Vasconcellos